



**ICSV20**  
**Bangkok, Thailand**  
**7-11 July 2013**

# **THERMAL AND FLUID DYNAMIC ANALYSIS OF PARTIALLY PREMIXED TURBULENT COMBUSTION DRIVEN BY THERMO ACOUSTIC EFFECTS**

Mina Shahi<sup>\*</sup>, Jim.B.W. Kok, Artur Pozarlik

*University of Twente, Faculty of Engineering Technology, Laboratory of Thermal Engineering, Enschede, The Netherlands*

<sup>\*</sup> e-mail: [m.shahi@utwente.nl](mailto:m.shahi@utwente.nl)

Thomas Sponfeldner

*Department of Mechanical Engineering, Imperial College London, London, UK*

Thermo-acoustic instability can be caused by the feedback mechanism between unsteady heat release, acoustic oscillations and flow perturbations. In a gas turbine combustor limit cycles of pressure oscillations at elevated temperatures generated by the unstable combustion process enhance the structural vibration levels of the combustor. In this paper, the behavior of turbulent partially premixed flames in a laboratory-scale lean partially premixed combustor (called as LIMOUSINE combustor) operating on natural gas- methane fuel mixtures is studied by using CFD methods. Depending on the operating conditions, the flame shows a stable or an unstable behavior. In order to predict the frequency and magnitude of the thermo-acoustic instability, and also to capture the reacting flow physics within the combustor, the influence of operating conditions on combustion characteristics is examined by using unsteady three-dimensional RANS solution of the conservation equations. To understand the effects of operating conditions on the observed stability characteristics, the time averaged velocity fields were measured with Particle Image Velocimetry (PIV) for the thermo-acoustically stable and unstable operating conditions of the combustor. The comparison of the CFD calculations with the mean velocity fields shows good agreement. The results of the present study demonstrate the relationship between the flame structure, the mean velocity field and pressure fluctuations under different operating conditions.

## **1. Introduction**

In many theoretical models of turbulent combustion processes it has been assumed that either the fuel and oxidizer are fully premixed prior to the combustion or they enter to the flame zone separately. However, in reality, this is often not the case. Numerous practical combustion devices, including gas turbines often operate in a partially premixed burning regime in which the fuel and oxidizer are partially mixed at the time of combustion. Modelling such a complex combustion physics

numerically has been always a challenging task. Therefore the objective of this paper is to investigate the impact of operating conditions on the flow and flame dynamics in a laboratory-scale lean partially premixed combustor. A bluff body stabilization approach is of particular interest here. The recirculating flow region behind the bluff body contains hot combustion products that ignite the incoming reactants. Considering that the unsteady flow fields in reacting bluff-body flows are mainly dominated by large-scale coherent structures, even a small change in the flow field can modify hydrodynamics at the burner outlet by increasing/decreasing velocity of the oxidizer and fuel and in consequence affecting the strength of the recirculation zone. This can play an important role in the mechanisms of the flame stabilization and mixing, which may cause thermo-acoustic instabilities.

In this paper, the study is divided into three sections. The first section focuses upon instability mechanism. The second and third sections provide the information about the experimental configuration and numerical methods, respectively. The last section which is devoted to the results, represents the dynamic of the flame under a stable and an unstable condition.

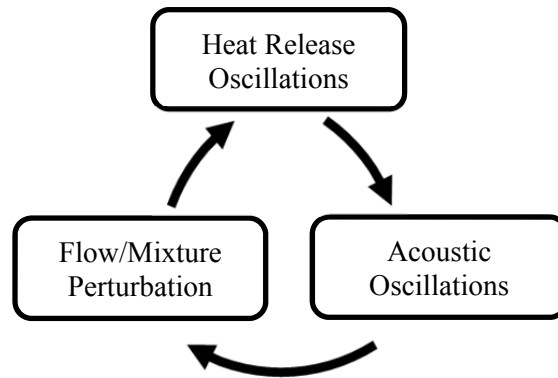


**Figure 1:** The feedback mechanism affecting the appearance of thermoacoustic instabilities in the combustion processes.

## 2. Thermoacoustic instability: Limit cycle feedback loop

Despite of the good emission performance, the lean premixed combustion of natural gas suffers from high sensitivity to thermoacoustic instabilities. The main phenomena involved in the feedback mechanism process are depicted in Fig. 1. This feedback process affects the appearance of the thermoacoustic instabilities. A wide range of involved dynamics promotes a resonant coupling between unsteady combustion processes, pressure field in the combustion system and the mixing process. Perturbations of heat release are part of a self-exciting loop initiating the thermoacoustic instability. Fluctuations of velocity, acoustic oscillations (i.e. fluctuation of pressure field), perturbations in the fuel concentration and in the mixing process may result in heat release perturbations and consequently pressure fluctuations. Depends on the phase shift between these dynamic systems, energy may be feed back into the initial perturbation source sustaining or damping the instability mechanism. The Rayleigh criterion <sup>[1]</sup> which recognizes the difference between damped or amplified interaction between pressure and heat release is often used to investigate and predict combustion instabilities. It states that if pressure and heat release fluctuations are in phase, the magnitude of thermoacoustic instabilities are enhanced, whereas the instabilities is damped when the pressure oscillations and heat release are out of phase. This criterion is expressed by the following Equation:

$$\iiint_{\Omega} p'q' d\Omega > 0$$

where  $p'$  and  $q'$  are pressure and heat release fluctuations, respectively, integrated over one cycle of the oscillation in the flow domain  $\Omega$ . The product of thermal oscillation and sound pressure fluctuation must be positive to enable combustion oscillations, whereas the negative sign indicates damping process. When the acoustic energy losses match the energy gain a stationary oscillatory

behaviour is obtained which is referred to as the limit cycle oscillation (LCO). Since the integrals are also spatial both effects: destabilizing and stabilizing can occur at different locations of the combustor and at different times. The overall stability of the combustor will be then defined by the net mechanical energy added to the combustor domain.

### 3. The burner description

The experiment, applied for the validation of numerical studies is performed on a test rig presented in Fig. 2. The set-up is designed to study limit cycle oscillations due to thermo-acoustic instability. The experimental research is performed at University of Twente and also four other laboratories associated within the framework of the European project LIMOUSINE.

The combustor consists of two rectangular ducts with different widths, with the burner coupling both ducts. The duct upstream of the burner has a  $25 \times 150 \text{ mm}^2$  cross section and is 275 mm long, whereas the duct downstream the burner has a  $50 \times 150 \text{ mm}^2$  cross sectional area to compensate the volume expansion due to the combustion. In the transition between the ducts a wedge-shaped bluff body which creates a flow recirculation is used to stabilize the flame. Since the width of the combustor (150 mm) is much larger than the depth (50 mm) but significantly smaller than the height, the test rig resembles a two-dimensional combustor. Details about dimensions of the model combustor are summarized in Table 1.

The combustor has four large quartz glass windows on each side of the burner to allow optical access to the flame stabilizing region. All pieces the combustors, except the brass bluff body, are made from heat resistant stainless steel S310.

Air as the oxidizer is injected at the upstream end through an air distribution system which consists of two longitudinal pipes with 2mm diameter holes. The fuel used here is bottled methane. From the side surfaces of the wedge gaseous fuel is injected through 62 holes. The burner can operate at a large range of power and air factors. Air and fuel flows are controlled via Bronkhorst mass flow rate controllers and Labview software. The dynamic pressure signal is recorded at 6 points along the combustor with piezoelectric pressure transducers. Three pressure transducers located in the plenum are flush mounted in the wall, while the pressure transducers located downstream the burner are mounted in side tubes for protection from high temperature. To assure anechoic boundary conditions, every side tube is connected to a long hose filled at the end with an acoustic damping material. Pressure signals are recorded with a six channel Labview data acquisition system (DAQ) linked to a PC. For every operating condition, 10k simultaneous samples are recorded at frequency of 3125 HZ.

The only cooling of the combustor is by natural convection and radiation. The LIMOUSINE test rig behaves like a variation of a Rijke tube<sup>[2]</sup>. It deviates from the standard Rijke tube because it is closed at the bottom end, open to the atmosphere at the downstream end and it has an air flow forced into it.

### 4. Numerical approach

Ansys CFX 14.0 uses an implicit finite volume formulation to construct the discretized equations representing the Reynolds Averaged Navier-Stokes equations for the fluid flow. The model consists of a compressible solver with co-located (non-staggered) finite volume method such that the control volumes are identical for all transport equations<sup>[3]</sup>. To avoid the decoupling of the pressure field, CFX uses the Rhie-Chow<sup>[4]</sup> discretization method for the mass terms as modified by Majumdar<sup>[5]</sup>. A coupled algebraic multi-grid solver is used to give robust solutions for the governing discrete system of linearized equations. For the discretization of governing equations, a high resolution advection scheme for spatial and second order backward Euler discretization for time accuracy is used. The computational geometry used in the solution process is illustrated in Fig. 3. Details about boundary conditions imposed on the domain are summarized in Table 2.

The closed acoustic inlet boundary condition at the upstream end was implemented by using a uniform and steady inlet velocity profile at the air inlet, which ensured an acoustically closed inlet.

The mass flow rate of fuel is specified at the fuel inlet. A reflecting boundary condition is applied at the outlet by setting pressure at that location to 1 atm, which implements the open acoustic boundary condition. In order to estimate the effect of heat losses through the walls, the walls were treated as convective boundaries; an outside heat transfer coefficient and outside temperature are specified.

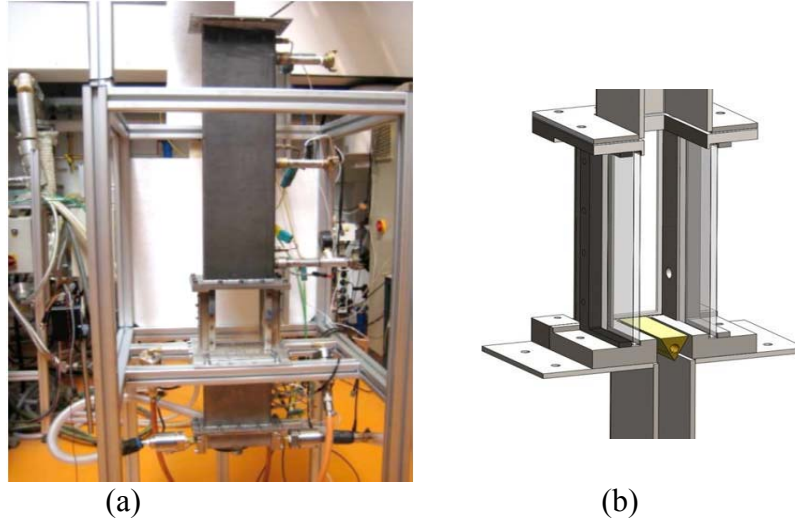


**Figure 2** : Experimental set up (a) and LIMOUSINE burner (b) .

**Table 1** : Dimensions of the model combustor.

Location	Dimension (mm)
Upstream height	220
Upstream width	25
Downstream height	780
Downstream width	50
Width of the combustor in the third direction	150

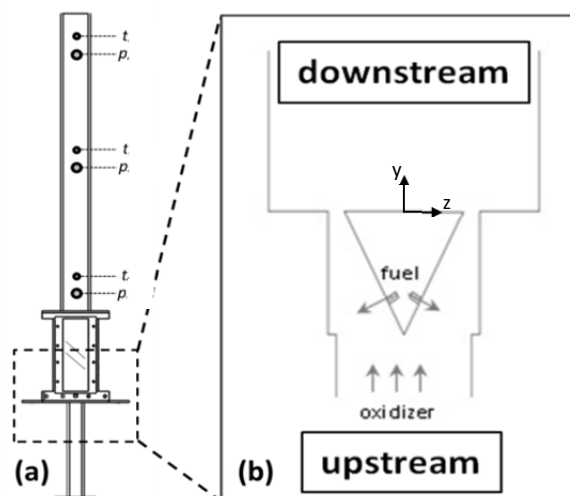


**Figure 3** : A schematic representation of the model combustor: computational domain in CFD calculation (a) and an enlarged view around the wedge (b).

The Shear Stress Transport Turbulence model (SST) <sup>[6]</sup> in the steady state calculations, and the Scale-Adaptive Simulation model (SAS) <sup>[7]</sup> for the transient calculations are used . Reacting flow simulations are carried out on the model combustor using the BVM combustion model as available in ANSYS CFX <sup>[8]</sup>.

**Table 2:** Boundary condition.

Location	B.C
Air Inlet	Normal speed
Fuel Inlet	Mass flow rate
Outlet	Average static pressure
Walls	Non-slip

## 5. Results and discussions

### 5.1 Velocity & Temperature field

The velocity field was measured with Particle Image Velocimetry <sup>[9]</sup>.The measurements were performed at Imperial College London. The recording frequency was 10Hz. Compared to other velocity measurement techniques such as the Laser Doppler Velocimetry (LDV), PIV is capable of measuring the two-dimensional flow field inside the combustor. This can be used, e.g. in order to visualize the recirculation zone behind the bluff body, which is an important factor for the flame stabilization mechanism in the LIMOUSINE combustor.

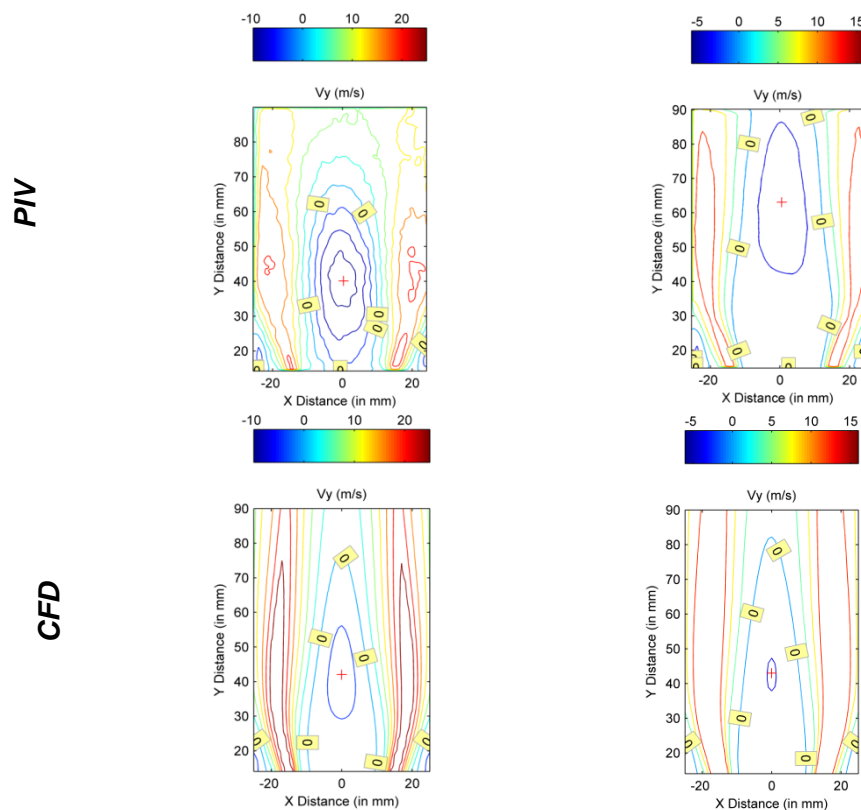


**Figure 4:** CFD & PIV data representing the average stream wise velocity component during : the unstable (left column) and the stable combustion (right column).

Figure 4 shows the mean vertical velocity component ( $v$ ) downstream of the bluff body for the unstable (left) and stable (right) operating point of the combustor. The experimental data has been averaged over 327 and 160 images, respectively for the unstable and stable flame condition which explains the reason for having rather noisy mean velocity fields. The origin of the vertical axis is the burner plane. In each part of this figure, isocontours of  $v = 0$  which represent the spatial boundaries of the recirculation zone are shown as well. For the unstable case, the simulation cap-



tured the correct trend but slightly over-predicted the magnitude of the streamwise velocity as well as the extent of the recirculation zone. For the stable operating condition of the burner the recirculation zone extends further downstream compared to the unstable flame and it is also less compact which results in a slightly wider recirculation zone compared to unstable case. Overall, there is fair agreement between the simulations and the measurements, which is important as the prediction of the reversal zone behind the bluff body is of a great importance for the subsequent analysis of the flame-flow interaction inside the LIMOUSINE burner.

The exchange between the recirculating hot exhaust gases and the fresh methane air mixture supplies the energy required to ignite the fresh gases. The shear layer between the hot exhaust gases and the fresh methane air mixture acts in a way to increase the temperature of the reactants as they are convected into the flame zone (see Fig. 5). Numerical and experimental data regarding the reattachment lengths for both flames have been compared; the calculation error is presented in Table 3 .

**Table 3:** the center of the recirculating zone location: presented in Fig. 4 by (+)

	$y_c$ (mm)		
	CFD	PIV	Error (%)
Stable flame	43	62	30
Unstable flame	42	40	5

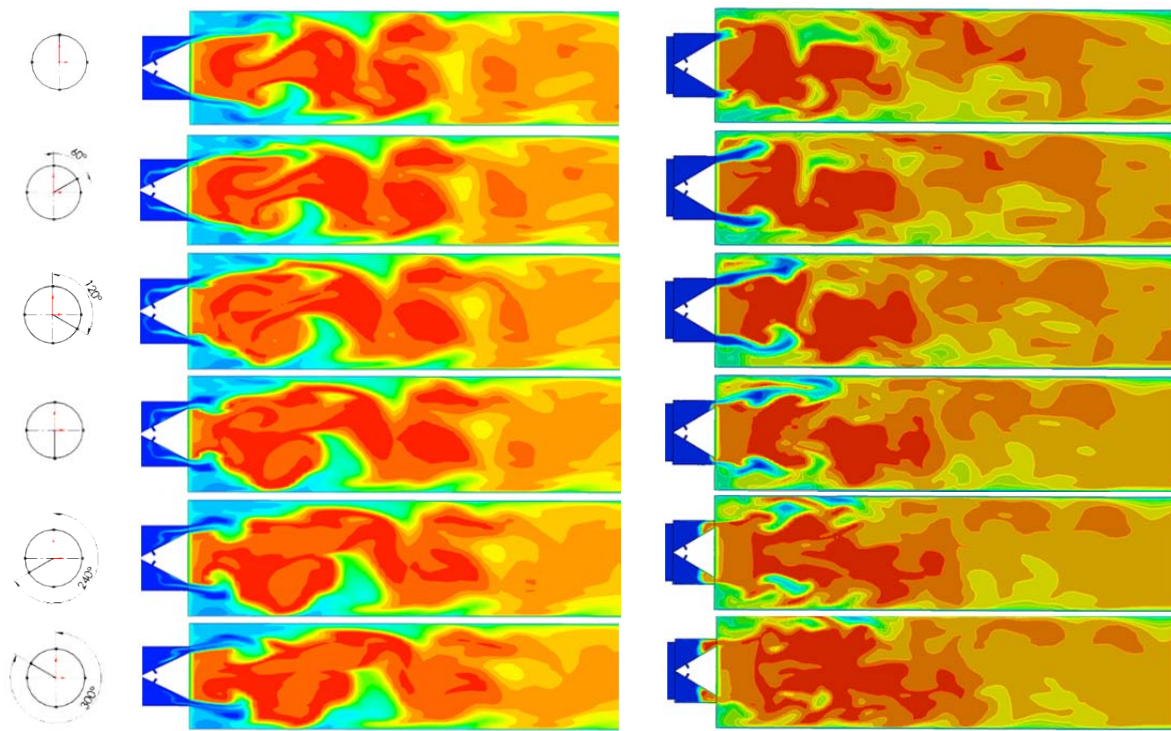


**Figure 5 :** instantaneous predicted temperature field (Over one cycle of oscillation) in the reacting flow at the middle plane ( $x=0$ ) for a stable (left column) and an unstable flame (right column)

Instantaneous numerical solution of the temperature fields are shown in Fig. 5 at six different phase angles for the stable and unstable regimes over one period of the first predicted mode. In both cases, the central recirculating zone (CTRZ), forms a flame stabilization region where the incoming mixture of air and fuel are mixed with the hot products before ignition. The recirculated hot combustion products transports momentum and energy back to the further upstream where they mix with the incoming fresh mixture. Furthermore, due to the sudden expansion of the combustor configuration, two corner recirculation zones (CRZ) are formed downstream of the bluff body. Presented temperature fields show that the unstable flame moves forward and backward during one cycle of oscillation. This movement, in the other words, the perturbation of the flow rate induced by the

standing mode, controls the reaction rate in front of the burner. Natural coherent structures in the shear layers lead to a penetration of the fresh gases to the flame before it burns completely, which also results in a fluctuating heat release rate. Due to the expansion of the flow the flame is pushed outward and simultaneously blocks the inlet flow causing the flame flashbacks periodically in the burner. Unburned mixture segments broken up away from the main stream of the flow, may generate local hot spots further downstream. The flame zone thus reaches the strongly burning state which is shortened and becomes compact compared to the stable regime.

## 5.2 Pressure field

The geometric enclosure of the combustor acts as a resonator. Pressure waves which are reflected at the boundaries of the burner may interact with the heat release process (see Fig.1). If the dissipation of acoustic energy within the chamber and also at the boundaries is smaller than the energy gained by the acoustic disturbances, pressure waves are excited and pressure amplitudes will soon grow up to a saturation limit which is referred to the limit cycle oscillations. This is shown in Fig. 6 for both: stable and unstable flame conditions.

Figure 7 represents variations of velocity and heat release in the combustor. Considering the unstable flame, this plot confirms that the unsteady reaction rate is controlled by the velocity oscillations, which are the source of strong movement of the flame observed in the Fig. 5.

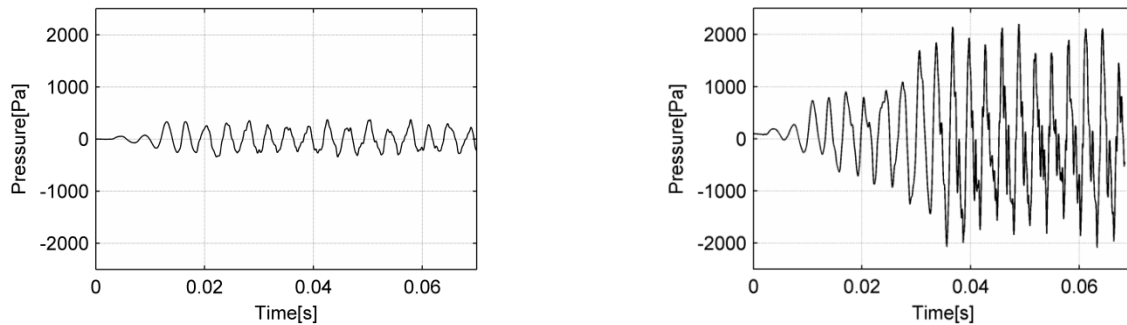


**Figure 6:** Time signals of pressure for the stable (Left column) and unstable flame (Right column).

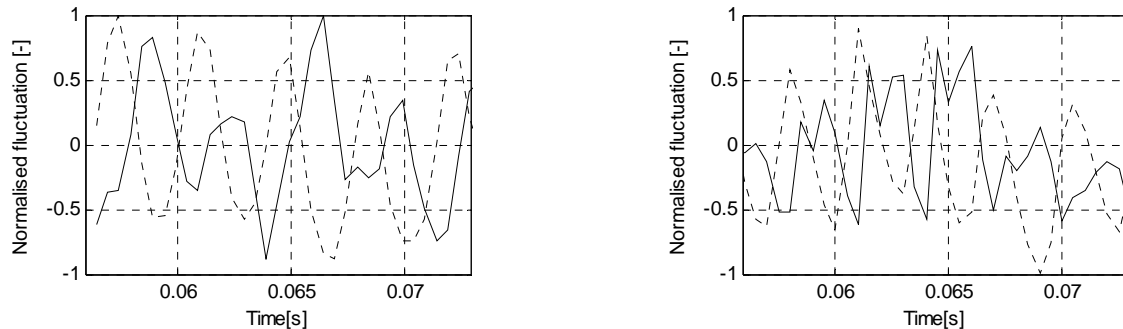


**Figure 7:** Velocity fluctuations through the burner (continues lines) and heat release fluctuations (dash lines) for the stable (left column) and unstable flame (right column)

Characterisation of the growth of the pressure amplitude is important for the life time assessment. The lifetime of the combustor may be significantly reduced because of the high amplitude instabilities occurrence. The actual pressure growth at one test case is hard to measure experimentally since the combustor is gradually progressed to reach the corresponding operating point either from another operating point or start-up period. Thus, the actual energy generated to grow the instability can be suppressed due to the energy stored from the previous operating mode. However the instability growth mechanism can be captured by the numerical model. The growth rate of the amplitude of pressure fluctuations is calculated and shown in Table 4. As it can be seen the growth rate (i.e. 'b') is changing depending on the location of the pressure transducer. It is also representing an alternating increase and decrease in the amplitude of the growth function (i.e. 'a') along the combustor pointing to the presence of the pressure nodes.

**Table 4:** Growth rate of pressure signal during LCO (Growth function =  $ae^{bt}$ )

	Thermal power (kW)	equivalence ratio	Pressure sensors	a	b
Unstable flame	35	0.77	P1	609.30	20.40
			P2	844.86	13.34
			P3	291.03	27.29
Stable flame	25	0.67	P1	325.89	-1.96
			P2	352.68	0.22
			P3	114.55	5.78

## Conclusions

The flame structure of an atmospheric bluff body stabilized burner fired with methane has been investigated as a function of thermal power and air/fuel equivalence ratio. In order to visualize the characteristics of the recirculation zone for the stable and unstable operating conditions of the LIMOUSINE combustor, the average flow field was predicted with unsteady RANS calculations and also measured with the PIV method. The results indicated more pronounced and stronger recirculating flow for an unstable flame causing the hot gases to be pushed past the wedge creating hot pockets upstream which could trigger/amplify acoustic oscillations. While the unstable regime is characterized by the high amplitude pressure oscillations, the amplitude of the signal in the stable regime is in the order of tenths of Pascal. In general it can be concluded that for an unstable flame the thermal energy released from chemical reactions is fed in to the acoustic fluctuations in the burner through a feedback mechanism including the mutual coupling between acoustics excitation, mass flow fluctuation, flame motion and heat release oscillation.

## Acknowledgments

The authors would like to acknowledge the funding of this research by the EC in the Marie Curie Actions Networks for Initial Training, under call FP7-PEOPLE-2007-1-1-ITN, Project LIMOUSINE with project number 214905. Special thanks go to Dr. Phil Stopford for the support in the use of ANSYS-CFX.

## REFERENCES

- <sup>1</sup> Rayleigh, J., The explanation of certain acoustic phenomena. *Nature*, **18**(455), 319-321, (1878).
- <sup>2</sup> Rijke, P.L., On the vibration of the air in a tube open at both ends. *Philosophical Magazine*, **17**, 419-422, (1859).
- <sup>3</sup> Patankar, S.V., Numerical Heat Transfer and Fluid Flow, *Hemisphere Publishing Corp*, (1980).
- <sup>4</sup> C.M.Rhie and W.L.Chow, a numerical study of Turbulent Flow Past an Isolated Airfoil with the Trailing Edge Separation. *Aiaa Journal*, **21**(11), 82-0998, (1982).
- <sup>5</sup> Majumdar, S., role of underrelaxation in momentum interpolation for calculation of flow with nonstaggered grids. *Numerical Heat Transfer*, **13**(1), 125-132, (1988).
- <sup>6</sup> Menter, F.R., 2-Equation Eddy-Viscosity Turbulence Models for Engineering Applications. *Aiaa Journal*, **32**(8), 1598-1605, (1994).
- <sup>7</sup> Menter, F.R. and Y. Egorov, The Scale-Adaptive Simulation Method for Unsteady Turbulent Flow Predictions. Part 1: Theory and Model Description. *Flow Turbulence and Combustion*, **85**(1), 113-138, (2010).
- <sup>8</sup> ANSYS (2010). *Release 11.0 Documentation for ANSYS*.
- <sup>9</sup> Raffel, M., et al., Particle Image Velocimetry: A Practical Guide, *Springer*, London, (2007).